ELSEVIER

www.elsevier.nl/locate/jorganchem

Journal of Organometallic Chemistry 602 (2000) 75–90

Journal of Organometallic Chemistry

Electrochemistry of ruthenium metallocenes☆ Part 3. Synthesis and properties of ruthenium [2_2]paracyclophane complexes with methacrylic acid and methacrylate ester substitutents

Bernhard Gollas [a,1], Bernd Speiser [a,*], Ioannis Zagos [a], Cäcilia Maichle-Mössmer [b]

[a] *Institut für Organische Chemie, Universität Tübingen, Auf der Morgenstelle 18, D-72076 Tübingen, Germany*
[b] *Institut für Anorganische Chemie, Universität Tübingen, Auf der Morgenstelle 18, D-72076 Tübingen, Germany*

Received 3 January 2000; accepted 14 February 2000

Dedicated to Professor Virgil Boekelheide on the occasion of his 80th birthday

Abstract

Four [2_2](1,4)cyclophanes bearing one or two methacrylate ethyl ester and methacrylic acid substituents and ruthenium arene complexes of these compounds are synthesized. The structure of the ligands and the complexes is characterized by NMR spectroscopic techniques. For some of the ligands X-ray crystal structure analyses support the assignments. The mono-substituted [2_2](1,4)cyclophanes prefer to form anti-complexes, with the Ru central atom bound to the unsubstituted aromatic deck. The irreversible electrochemical oxidation of the cyclophanes is studied by cyclic voltammetry, and, in contrast to mono- and divinyl[2_2](1,4)cyclophanes does not produce permanent films on the electrode. The electrochemical reduction of the complexes proceeds as a two-electron process and produces the kinetically stable corresponding Ru^0 species. The anodic oxidation of the title compounds is irreversible and leads to filming of the electrode surface. © 2000 Elsevier Science S.A. All rights reserved.

Keywords: Ruthenium complexes; Cyclophanes; NMR spectroscopy; Cyclic voltammetry; Electrode modification

1. Introduction

Various classes of sandwich-type organometallic complexes with ruthenium as the central atom have been characterized with respect to their redox properties. Those with cyclopentadienyl ligands (e.g. ruthenocene [2]) have been known for a long time (for recent examples of analogues and derivatives, see e.g. [3–6] and references therein). The corresponding Ru arene complexes with benzenoid 6π-electron donor ligands were made reasonably available by Bennett's synthesis [7,8].

Ruthenocene is oxidized in a chemically reversible one-electron step to the ruthenicinium ion [9,10], or in an overall two-electron ECE type sequence in coordinating electrolytes [9,11]. In contrast, the prototype compound bis(HMB) ruthenium (II) (**1**), with η^6-ligands [12] (HMB = hexamethylbenzene; in all formulae of the complexes, the counter anions have been omitted) is reduced in a two-electron reaction [13–15] to the corresponding Ru^0 complex with a fluctuating structure [12] and one η^6-HMB ligand converted to a η^4-HMB unit [12,16].

Aside from substituted benzenes [12,17,18] and polycyclic aromatic compounds [19,20] also [2_n]cyclophanes have been employed as arene ligands in Ru^{2+} complexes [13,21–24] (see, e.g. **2** and **3**). Such compounds were discussed as models for polymetallocenes with possibly interesting electronic properties [24] due to the close distance and the resulting strong electronic interaction between the aromatic decks in the cyclophane

☆ Part 2, see Ref. [1].

* Corresponding author. Tel.: +49-7071-2976205; fax: +49-7071-295518.

E-mail address: bernd.speiser@uni-tuebingen.de (B. Speiser)

[1] Present address: Department of Chemistry, University of Southampton, Highfield, Southampton, SO17 1BJ, UK.

0022-328X/00/$ - see front matter
PII: S0022-328X(00)00121-2

ligand [25–27]. Most recently, work has been extended to [3_n]cyclophanes as ligands in organometallic Ru^{2+} complexes [28].

Ru-cyclophane complexes are advantageously prepared by Boekelheide's variation of the Bennett synthesis [24,29,30], except for special cases with high electron densities in the rings [23] where the original Bennett procedure suffices. In general, the redox chemistry of these complexes seems to be similiar to that of **1** and various factors influencing the redox potentials have been discussed [24,30].

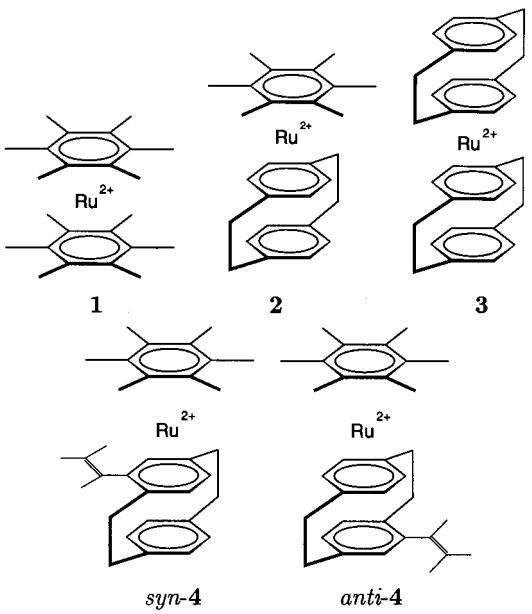

1 **2** **3**

syn-**4** *anti*-**4**

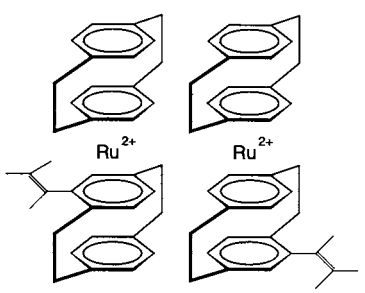

syn-**5** *anti*-**5**

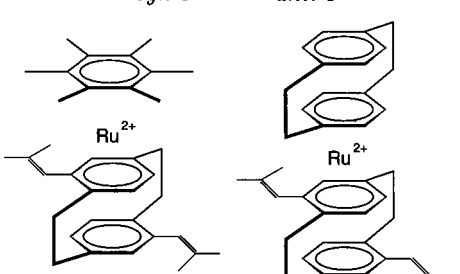

6 **7**

We have recently described Ru^{2+} complexes with ethenyl-substituted [2_2](1,4)cyclophane ligands [31], e.g. **4**–**7**. The synthetic protocol was slightly changed, since CF_3COOH used as a catalyst and solvent in the Bennett [7] and Boekelheide [24] syntheses caused side reactions at the ethenyl group. Cyclic voltammetry confirmed two-electron reduction of the ethenyl-substituted complexes [1,31,32], as in the unsubstituted parent molecule. However, additionally, oxidation signals were observed in the current/potential curves [31].

Ethenyl substitution of [2_2](1,4)cyclophane results in electropolymerizable styrene analogues [33]. In the framework of a proposed solid phase electrosynthesis of polymetallocenes [31], it is also essential that the ethenyl-substituted complexes such as **4**–**7** can be polymerized. This reaction is currently explored in our group.

We now extend our earlier work to the synthesis and characterization of Ru^{2+} complexes with η^6-[2_2](1,4)cyclophane ligands bearing ethenyl groups with polar, electronwithdrawing substituents. In particular, the cyclophane aromatic decks will be substituted by one or two ethyl methacrylate or methacrylic acid group(s). Preparation of such complexes requires the synthesis of new substituted [2_2](1,4)cyclophanes, **8a,b** and **9a,b** as ligands and their reaction with Ru-complex precursors to yield compounds **10**–**13**. In this paper also the NMR-spectroscopic analysis and electrochemical properties of complexes **10**–**13** are also described.

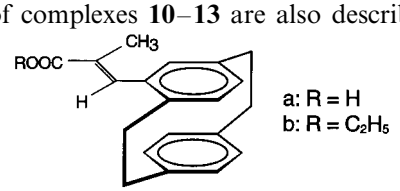

8

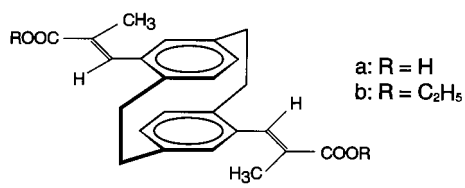

9

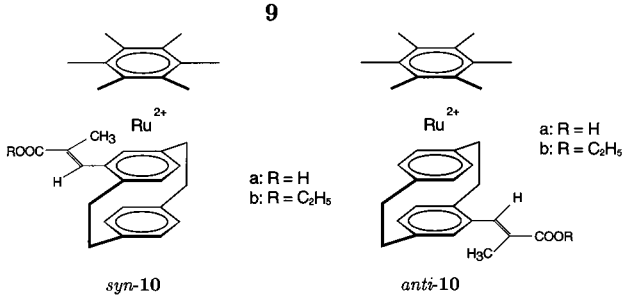

syn-**10** *anti*-**10**

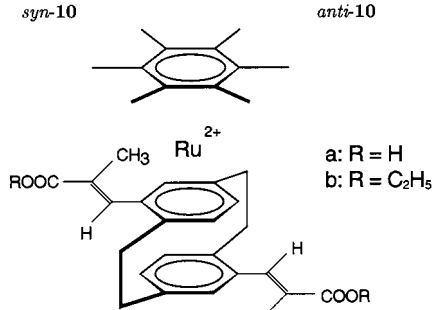

11

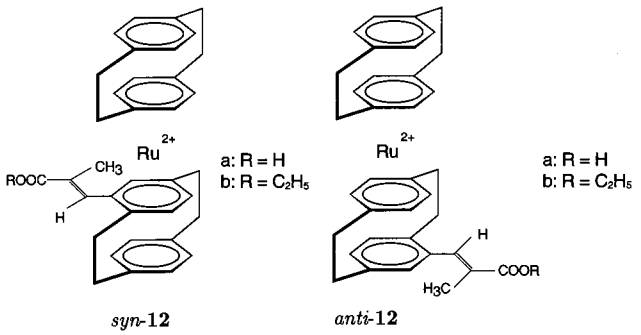

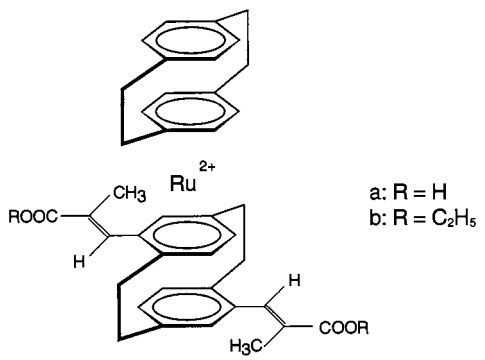

13

2. Results and discussion

2.1. Syntheses of ligands

Ligands used in the present work were synthesized according to Scheme 1 from aldehydes **14** or **16** in analogy to the preparation of 4-ethenyl-[2_2](1,4)-cyclophane (**15**) and the diethenyl compound **17** by Hopf and coworkers [34]. Triethyl-2-phosphonopropionate was used as the Wittig reagent [35], and the resulting esters **8b** and **9b**, respectively, were hydrolyzed by aqueous base to yield the carboxylic acids **8a** and **9a**. An excess of the Wittig reagent provided for yields above 80%. For an equimolar amount of the reactant as compared to the formyl precursor, the isolated yield of **8b** decreased to 54%.

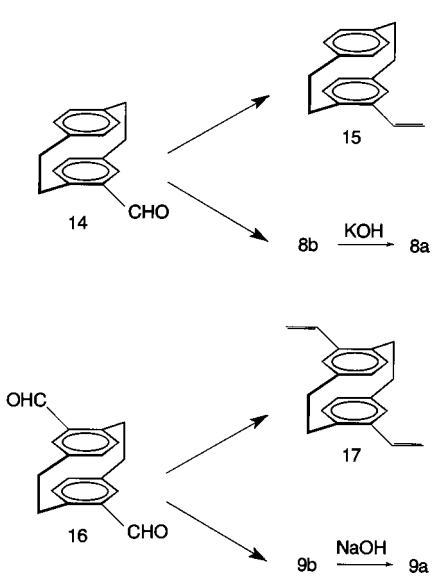

Scheme 1. Synthesis of ethenyl substituted [2_2](1,4)cyclophanes.

The mono-substituted compounds **8a**,**b** exhibit planar chirality and, since racemic monoaldehyde was used as the starting compound, a racemic mixture of the enantiomers is expected. We did not attempt to separate the stereoisomers. The 4,12-di-substituted cyclophanes **9** (pseudo-*para* isomers) are achiral molecules.

Furthermore, however, the Wittig reaction may result in two isomers with *E* or *Z* configuration at the newly created double bond. In all cases only the *E* isomer is formed as indicated by the NMR data and the X-ray crystal structure analyses (see below).

2.2. NMR spectroscopic characterization of ligands

The ^{1}H- and ^{13}C-NMR spectra of the cyclophanes **8a,b** and **9a,b** support the structures shown. The signals were assigned from either their chemical shifts (estimated from increment tables) [36], from consideration of the splitting patterns and the coupling constants resulting from spin–spin coupling, or from H,H- and C,H-COSY spectra. Finally, results from earlier work [31] for cyclophanes **15** and **17** were used as reference values.

The spectra of the centrosymmetric, disubstituted cyclophanes **9a,b** are composed of spin systems related to the vinyl group, the two aromatic decks, the ethano bridges and the ester or carboxylic group. Most signals are analogous to those in the spectra of **17** [31], and are consistent with the expected symmetry of the pseudo-*para* disubstituted [2_2](1,4)cyclophanes.

Strong effects of the substitution are, however, expected in the vinyl moieties. Indeed, the C_α-proton resonance in the substituent shifts from δ 6.8 ppm (**17**) downfield by almost 1 ppm in **9b**, and further by 0.56 ppm (**9a**, in d_5-pyridine). Coupling of the vinyl proton with the methacrylic CH_3 protons yields a doublet ($J = 1.4$ Hz) for the latter. The reverse effect on the signal of the single vinyl proton could not be resolved. The signal of the carboxylic proton in **9a** could not be observed in d_5-pyridine, probably due to fast exchange reactions. However, it appears at 12.52 ppm in d_6-DMSO.

Similar to **15** as compared to **17**, the spectra of the monosubstituted cyclophanes **8a,b** are more complex than those of **9a,b**. They are composed of the spin systems of the vinyl group, the substituted and the unsubstituted aromatic decks, the two different ethano

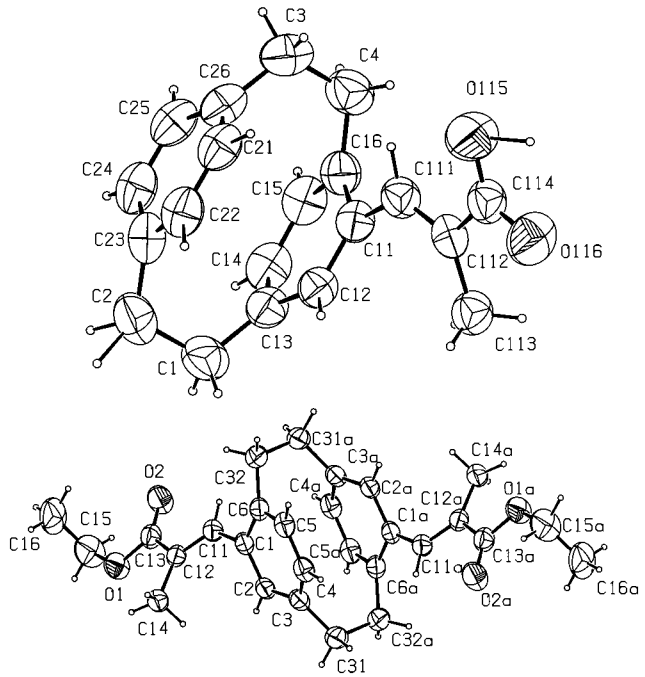

Fig. 1. Crystal structures of compounds **8a** (top) and **9b** (bottom).

bridges, and the ester or carboxylic acid group. As in the case of **9a** and **9b** most resonances appear at values expected from a comparison to the spectra of **15**. A NMR spectrum of **8a** in d_6-DMSO shows the COOH-proton at δ 12.48 ppm, similar to the one of the di-carboxylic acid, indicating that the changes of the chemical shifts between the mono- and the disubstituted compounds are minor.

Increment calculations [36] were used to predict the signal of the vinyl proton in the *E* or *Z* configurations with a phenyl substituent as a model for the [2$_2$](1,4)cyclophane group. For the *Z* isomer a resonance in the region of $\delta \approx 7.0$–7.14 ppm is expected, which is not observed in the ^{1}H-NMR spectra of the products. On the other hand, the signal at $\delta \approx 7.6$ ppm as estimated for the *E* isomer is found in the spectra of all four compounds. An analysis of the allylic coupling constants which could in principle also distinguish between *E* and Z isomers was not conclusive.

The ^{13}C results for the cyclophanes synthesized in the present work follow the general behaviour deduced from the ^{1}H-NMR spectra and are in accordance with the proposed structures.

2.3. X-ray crystal structures of ligands

The X-ray crystal structure of mono-ester **8b** has already been published [37]. Results of X-ray crystal structure analyses for **8a** and **9b** are shown in Fig. 1 as well as Table 1.

They clearly point out the formation of the *E* isomers at the vinylic double bond as concluded from the NMR spectra. The aromatic decks of the cyclophanes are tilted out-of-plane by up to 13.8°. The out-of-plane deviations of the bridgehead carbons adjacent to the substituent are larger than those of the other aromatic carbons. This is similar to the distortion in monoester [37] **8b** and slightly larger than in the parent compound, [2$_2$](1,4)cyclophane (12.6°) [25].

2.4. Electrochemistry of ligands

In earlier experiments [31,33] the ethenyl-substituted [2$_2$](1,4)cyclophanes **15** and **17** had shown oxidation peaks in cyclic voltammograms at considerably lower oxidation potentials than the unsubstituted parent molecule [38].

Fig. 2 shows cyclic voltammograms of the vinyl derivatives **15** and **17** (as comparison) as well as those

Table 1
Crystal structure data of [2$_2$](1,4)cyclophanes **8a** and **9b**

	8a	**9b**
Molecular formula	$C_{20}H_{20}O_2$	$C_{28}H_{32}O_4$
Molecular weight	292.36	432.54
Wavelength/Cu–K$_\alpha$ (Å)	1.54184	1.54184
Temperature (K)	233(2)	233(2)
Space group	*C*2/*c* (No. 15)	Monoklin/$P2_1/c$ (No. 14)
Unit cell dimensions		
a (Å)	38.967(10)	12.651(2)
b (Å)	11.3356(13)	11.2492(12)
c (Å)	8.017(2)	8.201(2)
α (°)	90	
β (°)	95.707(10)	90.170(10)
γ (°)	90	
V (Å^3)	3499.1(12)	1167.1(4)
Z	8	2
D_{calc} (Mg m^{-3})	1.110	1.231
Absorption coefficient (mm^{-1})	0.553	0.643
F(000)	1248	464
Color	Colorless	Colorless
Habit	Needle	Bloc
Crystal size (mm)	0.60 × 0.30 × 0.30	0.35 × 0.25 × 0.25
Theta range (°)	5.21–66.05	5.26–64.85
Index ranges	$-1 \le h \le 45$ $0 \le k \le 13$ $-9 \le l \le 8$	$-14 \le h \le 14$ $0 \le k \le 13$ $-1 \le l \le 9$
Reflections collected	3123	2424
Independent reflections	2985 [$R_{int} = 0.0308$]	1978 [$R_{int} = 0.0316$]
Reflections observed	2156	1819
Criterion for observation	$>2\sigma(I)$	$>2\sigma(I)$
Data/restraints/parameters	2985/0/280	1978/0/146
Final *R* indices [$I > 2\sigma(I)$]	$R_1 = 0.0782$, $wR_2 = 0.2252$	$R_1 = 0.0666$, $wR_2 = 0.1860$
Goodness-of-fit on F^2	1.102	1.062
Final *R* indices (all) R_1/wR_2	0.0988/0.2527	0.0705/0.1929
Extinction coefficient	0.0012(4)	0.014(2)
Largest difference peak and hole (e Å^{-3})	0.641 and −0.254	0.584 and −0.535

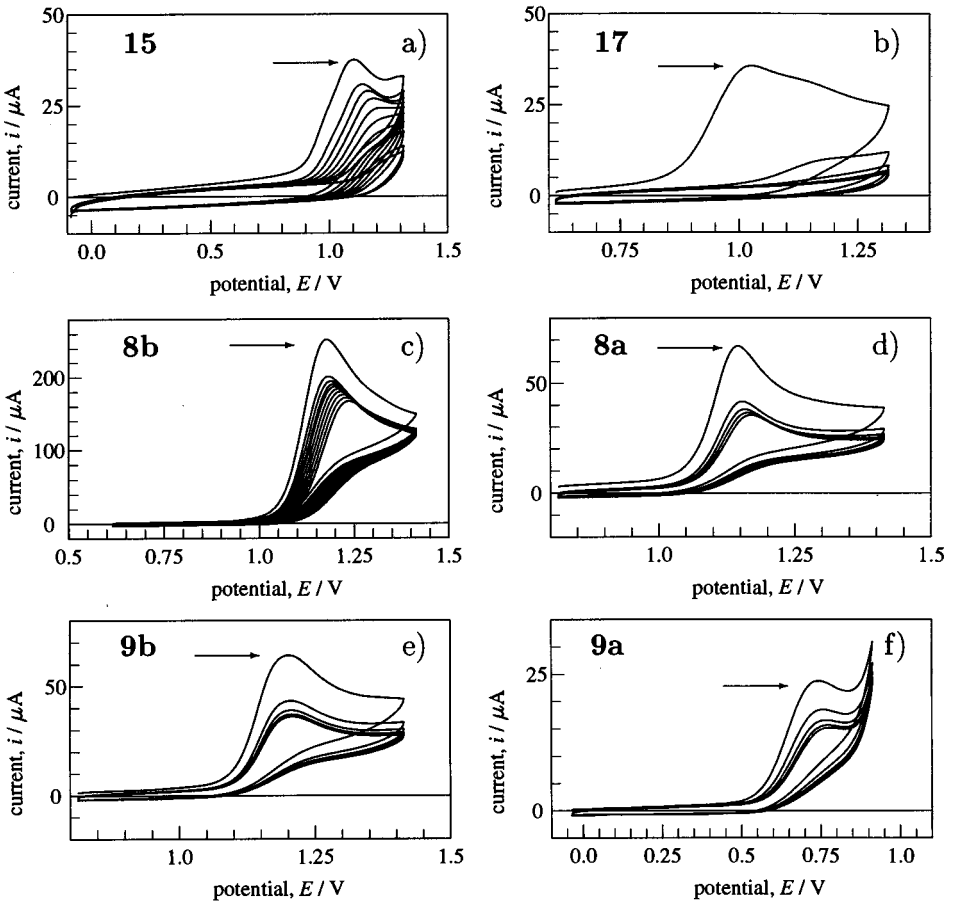

Fig. 2. Multi-cycle voltammograms of cyclophanes **15** (a; $c = 0.8$ mM), **17** (b; $c = 0.5$ mM), **8b** (c; $c = 4.0$ mM), **8a** (d; $c = 1.0$ mM), **9b** (e; $c = 1.0$ mM), **9a** (f; $c = 0.5$ mM); scan rate: $v = 0.1$ V s^{-1}, electrolyte: CH_3CN/0.1 M NBu_4PF_6, (except for **9a**: DMSO/0.1 M NBu_4PF_6), electrode material: GC; all potentials given versus fc/fc^+ in the respective solvent; first cycle indicated by arrow.

of the compounds **8a,b** and **9a,b**. Peak potentials recorded during the first oxidation scan (indicated by arrows in Fig. 2) are given in Table 2. Similar to **15** and **17**, the methacrylate ester and methacrylic acid substituted cyclophanes **8a,b** and **9b** exhibit irreversible oxidation peaks at $E_p \approx +1.2$ V in acetonitrile. These potentials are somewhat more positive than those for the vinyl substituted compounds, in accordance with the electron withdrawing effect of the carbonyl substituents. However, the effect on the peak potentials is only small.

It should be noted that the peak potentials in these chemically irreversible voltammograms are determined by a combination of thermodynamic and kinetic contributions, which cannot easily be separated. This is also a possible reason for the unusually low peak potential for the oxidation of **9a** (in DMSO, due to solubility reasons) as compared to the other compounds investigated.

For **15** and **17**, during repeated potential cycling the peaks decrease in intensity until they finally disappear (Fig. 2a,b). This was explained by the formation of insoluble, dielectric oligomers which precipitate and block the electrode from further electron transfer [31,33]. Mono-ester **8b** also shows a decrease of the peak current during multisweep cyclic voltammograms in acetonitrile (Fig. 2c) and propylene carbonate (PC). The peak current decreases with increasing number of potential cycles, while the peak potential shifts to more positive values. The current decrease is, however, less pronounced as compared to **15** and, in particular, **17**. Furthermore, the blocking of the electrode surface, which was permanent for **15** and **17**, is only temporary

Table 2
Cyclic voltammetric peak potentials [a] of substituted [2₂](1,4)cyclophanes **8**, **9**, **15**, and **17**

Compound	E_p (mV)
15	+1103
8a	+1171
8b	+1197
17	+1017
9a	+759
9b	+1169

[a] All values referred to the fc/fc^+ redox couple; $v = 0.1$ V s^{-1}; GC electrodes; solvent: CH_3CN, except for **9a**: DMSO; supporting electrolyte: NBu_4PF_6, 0.1 M.

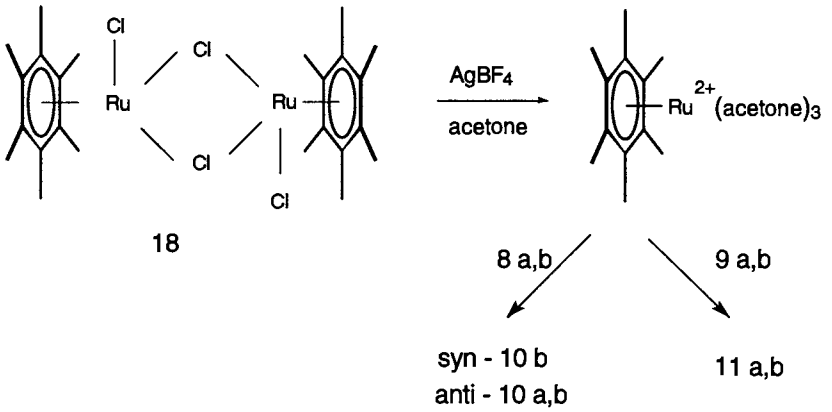

Scheme 2. Synthesis of HMB ruthenium complexes with ethenyl substituted $[2_2]$(1,4)cyclophane ligands.

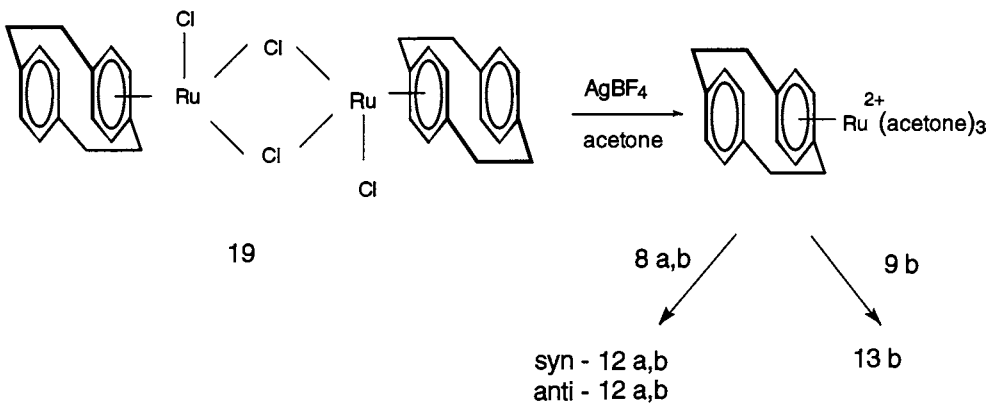

Scheme 3. Synthesis of $[2_2]$(1,4)cyclophane ruthenium complexes with ethenyl substituted $[2_2]$(1,4)cyclophane ligands.

in the case of the more polar **8b**. After keeping the filmed electrodes in the electrolyte for a period of several minutes, the voltammetric currents do increase again. Obviously, precipitated oligomers re-dissolve into the electrolyte. This may be due to the polar substituents, which increase the solubility of such products.

For **8a**, **9a**, and **9b** even during multiple potential cycles, the oxidation peak does not disappear. The slight decrease of the peak current is similar to that observed for a soluble redox couple and due to the depletion of the starting compound within the diffusion layer near the electrode. The peak potential does not significantly shift with the cycle number. The even higher polarity of oligomeric products could prevent their precipitation altogether. Alternatively, totally different products may be formed in these cases by the irreversible reaction of the primary oxidation products.

No reduction peaks of **8a,b** and **9a,b** are observed down to ca. -1.9 V. Only in the case of **9a** in a DMSO electrolyte, the potential window could be extended to more negative potentials. Under these conditions, an irreversible reduction peak was found in the voltammogram at $E_p \approx -2.3$ V.

2.5. Syntheses of ruthenium complexes

The synthesis of the HMB-Ru and the $[2_2]$(1,4)cyclophane–Ru complexes (**10** and **11** as well as **12** and **13**, respectively) follows the reaction sequences in Schemes 2 and 3. The bis(μ-chloro) complexes **18** and **19** have been described earlier [24,39]. The corresponding Ru acetone solvates form upon reaction with $AgBF_4$ under simultaneous precipitation of insoluble AgCl. The solvates in turn were treated with the cyclophanes **8** and **9** which displace the solvent molecules and act as 6-π-electron donors. Thus, 18 e^- complexes are formed. The ligands with electron-withdrawing substituents used in the present work are less reactive with respect to the replacement of the solvent molecules than their ethenyl analogues [31]. Thus, in some cases longer reaction times had to be applied than in the syntheses of **4**–**7**. In particular, the synthesis of **11a** required an exceptionally long reaction time, due to the low solubility of the substituting ligand **9a** in acetone.

Ligands **8** and **9** were used as the *E* isomers, and this configuration is also found in the resulting complexes (NMR). However, for the mono-substituted cyclophanes, upon complexation an additional possibility

for isomer formation exists: the substituent may be bound to the same deck to which the Ru central atom is attached (*syn*), or to the opposing one (*anti*). In most cases, mixtures of these regioisomers were formed, with the *anti*-isomer in excess. Only reaction of **8a** with the HMB-Ru solvate yielded pure *anti*-**10a** after a single crystallization. From the isomeric mixture *syn*/*anti*-**10b**, pure *anti*-**10b** was separated by repeated crystallization. Unfortunately, none of the Ru complexes gave crystals of a quality suitable for X-ray crystal structure analysis. Thus, the assignment of the regioisomers is based on the NMR spectra (see below). The regioselectivity of the complexation is explained by electronic (lower basicity of aromatic deck bearing the electron withdrawing substituent) and/or steric reasons.

2.6. NMR spectroscopic characterization of ruthenium complexes

Ru arene complex ^{1}H- and ^{13}C-NMR spectra, in particular from 2D techniques, have proven useful for the elucidation of structural details [23,24,29–31]. Based on these results, capping of a cyclophane such as **8** or **9** with one Ru^{2+} unit should result in characteristic changes of the chemical shifts of protons and ^{13}C nuclei. Furthermore, for the 4,12-disubstituted ligands **9a,b**, loss of the centro-symmetry is expected, since the two aromatic decks become different upon complexation. In the case of the mono-substituted cyclophanes **8a,b** the possibility of *syn*/*anti*-isomerism occurs (see above). These structural features of the complexes synthesized in the present work will be discussed in the following.

The derivatives of **9a,b** will be treated first. Generally, in the ruthenium complexes of cyclophanes two groups of proton signals for the aromatic decks are observed. Compared to the uncapped cyclophane spectra, one of them moves upfield by about 0.5 ppm, whereas the other shifts $\approx$0.5 ppm downfield. In earlier papers the high field signals were assigned to the deck complexed with Ru^{2+}, while the low field signals were attributed to the uncapped deck [23,29,31]. This behavior was rationalized by various factors including changes in bond order, ring current and electron density as well as the influence of the magnetic anisotropy of the ruthenium atoms [29]. Complexes **11** and **13** behave exactly in this way.

Strong effects were observed also for the ^{13}C-NMR resonances of the aromatic carbons in the capped (40–45 ppm upfield shift) deck, while only a moderate shift of a few ppm seems to be characteristic for the carbon atoms in the uncapped deck. This is again in accordance with earlier results [31].

Complexation additionally affects the chemical shifts of atoms in the vinyl groups attached to the cyclophane ligand. In the present cases, the vinyl protons and the three protons of the methacrylic methyl groups show significant differences, depending on the position of the substituent in the molecule. For example, the vinyl-H resonance in **9b** (δ 7.68 ppm) splits into two signals at δ 7.72 and 7.01 ppm in complex **11b**.

^{1}H-^{1}H-COSY experiments allowed to determine the connectivity between the vinyl protons and the respective deck. It appears that the vinyl proton signal of **11b** at δ 7.72 ppm correlates with the signal of the aromatic proton *ortho* to the methacrylic substituent of the downfield shifted *anti*-deck. On the other hand, the proton signal shifted upfield (δ 7.01 ppm) correlates with that of the *ortho*-proton of the *syn*-deck.

Correlation between the vinyl and the methyl proton signals in **11b** finally fixed the assignment of the chemical shifts of the CH_3 groups in the substituents (*anti*: δ 1.87 ppm; *syn*: δ 2.51 ppm).

This observation was especially useful for the interpretation of the spectra of the monosubstituted ruthenium complexes. In particular, it allowed the establishment of the regioselectivity of the capping reaction. From the mixture of regioisomers of **10b** one component could be isolated with high purity. The proton NMR signals of this compound led to the assignment as *anti*-**10b**, based on the chemical shifts and the correlations of the aromatic, vinyl and methacrylic CH_3 proton signals, as discussed above for the *anti*-deck substituent in disubstituted **11b**. Analysis of the additional signals in the spectra of the *syn*/*anti* mixture before recrystallization provided unequivocal shift values for the protons in *syn*-**10b**. From the spectrum of this mixture, it was also apparent that the HMB methyl proton chemical shift was affected by the presence of a *syn* (δ 2.46 ppm) or an *anti*-substituent (δ 2.53 ppm) in the complex. The integrals of the vinyl-, methacrylic methyl, and (with the highest accuracy) the HMB methyl signals for the two isomers could be used to determine the ratio of the *anti*- and *syn*-product yields. As mentioned already, the *anti*-products are formed preferredly.

The reasoning outlined above was then used to assign the signals of the regioisomers and to determine the isomer yield ratios in **10a** (only *anti* formed), **12a**, and **12b** (*anti* preferred in both cases).

Ru complexation decreases the chemical shift difference between the two C=C carbons in the cyclophane substituents. In general, however, the effect of the metal fragment is much less than observed earlier for vinyl substituents [31]. In no case crossing of signals occurs, which we had found in **4**, **6**, and **7** as being characteristic for *syn*-vinyl groups. Still, the carbon atoms in the methacrylic substituents show characteristic differences, depending on the positions of the substituents within the complex. For example, in **11b** the ^{13}C-NMR signals of the atoms attached directly to the aromatic deck (α) shift from 126.54 to 136.42 ppm if we compare the *syn*- and the *anti*-position, and a similar effect was observed for **11a**.

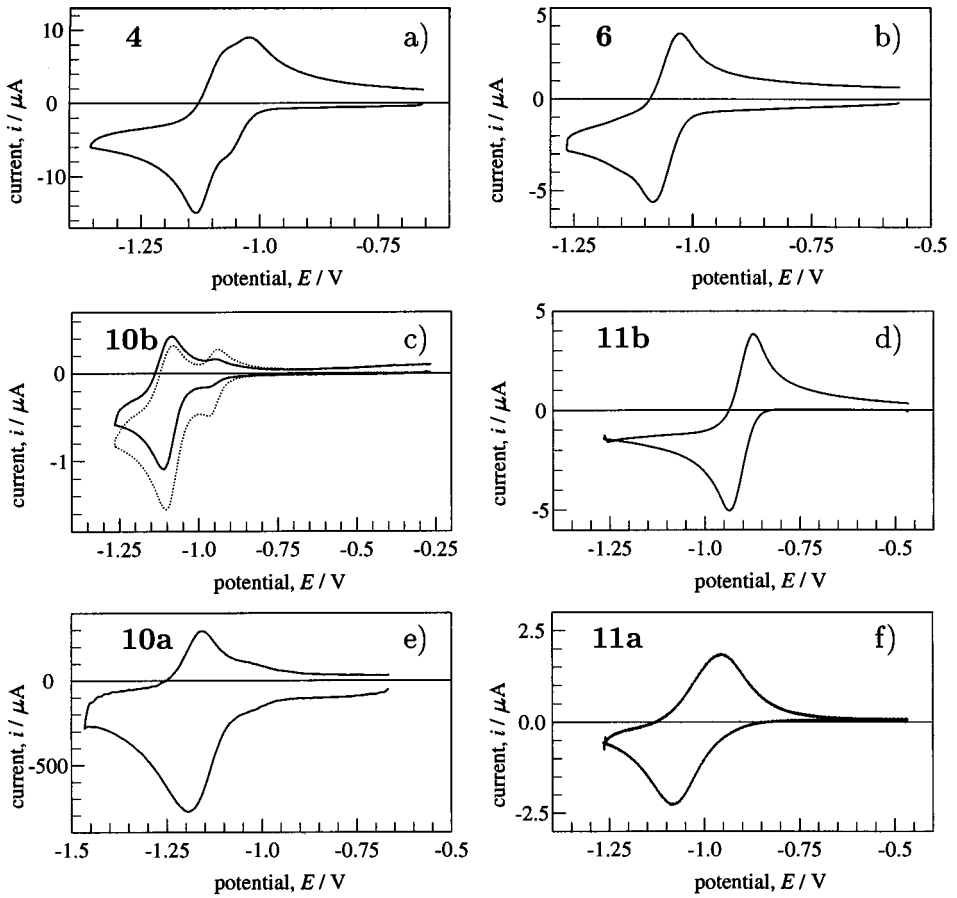

Fig. 3. Cyclic voltammograms for reduction of HMB ruthenium complexes; (a) *Syn*/*anti*-**4** in propylene carbonate/0.1 M NBu_4PF_6 at a Pt electrode, $v = 0.1$ V s^{-1}, $c = 0.89$ mM; (b) **6**; (c) *syn*/*anti*-**10b** [1:4.5 mixture (dotted line), *anti*-**10b** after recrystallization (full line)]; (d) **11b**, (e) *anti*-**10a**; (f) **11a**; **6**, 10, and 11 at a GC electrode; $v = 0.1$ V s^{-1} electrolyte: DCB/0.06 M NBu_4PF_6, $c = 0.5$ mM.

2.7. Electrochemistry of ruthenium complexes

All complexes synthesized can be reduced and oxidized at both Pt and glassy carbon electrodes. Here, we present results for the electrode reactions in *ortho*-dichlorobenzene (DCB) and propylene carbonate (PC) based electrolytes.

2.8. Reduction

Reductive cyclic voltammograms of the complexes at a glassy carbon (GC) electrode are shown in Figs. 3 and 4. Based on earlier reports [13,15,23,24,28,29,31] we assign the voltammetric signals to the two-electron redox process

$$Ru^{2+} + 2e^- \rightleftharpoons Ru^0 \quad (1)$$

In some Ru arene complexes fast follow-up reactions of the Ru^0 species had been observed [13,24,28]. In contrast, the cyclic voltammograms of **4**, **6**, and **10**–**13** indicate a high chemical reversibility of the reduction, and the Ru^0 species appear to be stable on the time scale used (scan rate $v = 100$ mV s^{-1}).

More detailed quantitative analyses of the cyclic voltammograms show [1,32] that the two formal potentials for the redox steps in reaction (1) have very close values. This gives rise to only a single peak couple in the current/potential curves. Voltammograms exhibiting two peak couples are due to the presence of two isomers. In the case of the isomeric mixtures the assignment of the voltammetric peaks to the individual *syn*/*anti* isomers was based on their relative intensity, which was compared to the isomer ratio determined from the NMR spectra of the respective sample. If no NMR data were available for the electrochemical sample, the relative potential shift was compared to that of a compound as similar as possible (e.g. **12b** and **10b**). Voltammograms clearly show enrichment of the anti-isomers during repeated crystallizations (Fig. 3c).

The voltammograms of the carboxylic acids *anti*-**10a** (Fig. 3e), **11a** (Fig. 3f), and **12a** (Fig. 4d) show distortions which are possibly due to adsorption or precipitation phenomena. Under the conditions employed here, the ester derivatives do not show such effects.

From the peak potentials we calculated mid-point potentials $\bar{E} = (E_p^{red} + E_p^{ox})/2$. Such potentials are listed

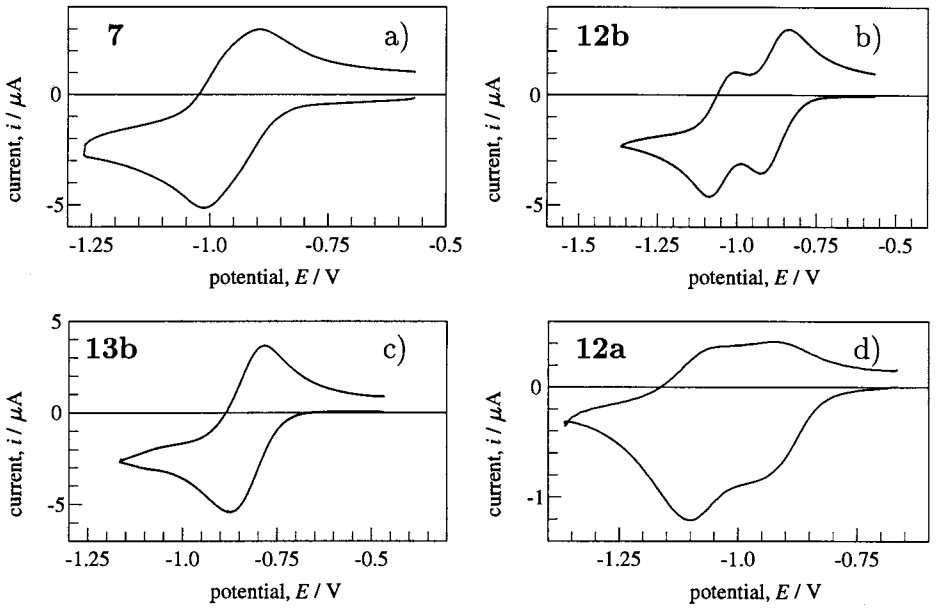

Fig. 4. Cyclic voltammograms for reduction of [2$_2$](1,4)cyclophane ruthenium complexes at a GC electrode; $v = 0.1$ V s^{-1}, electrolyte: DCB/0.06 M NBu_4PF_6, $c = 0.5$ mM; (a): 7; (b) *syn*/*anti*-**12b**; (c) **13b;** (d) *syn*/*anti*-**12a**.

Table 3
Mid-point potentials and peak potential differences in cyclic voltammograms for reduction of ruthenium arene complexes [a]

Complex [b]	$\bar{E}$ (mV)	ΔE_P [c] (mV)	Complex [d]	$\bar{E}$ (mV)	ΔE_p [c] (mV)	Complex [e]	$\bar{E}$ (mV)	ΔE_p [c] (mV)
2	−1100	42	**6**	−1056	57	*syn*-**4**	−1040	[f]
						anti-**4**	−1130	49
			11b	−904	63	*syn*-**10b**	−955	33
						anti-**10b**	−1091	41
			11a	−1019	127	*anti*-**10a**	−1176	33
3	−939	124	**7**	−955	114			
			13b	−829	90	*syn*-**12b**	−875	77
						anti-**12b**	−1047	81
						syn-**12a**	−938	45
						anti-**12a**	−1069	56

[a] At GC in DCB/0.06 M NBu_4PF_6; except for **2** and **3** (at GC in PC/0.1 MNBu_4PF_6) and **4** (at Pt in PC/0.1 M NBu_4PF_6); all values referred to the fc/fc$^+$ redox couple in the respective solvent.
[b] Complexes with unsubstituted cyclophane ligands, see also, ref. [24,29].
[c] Determined from experiments at $v = 0.1$ V s^{-1}.
[d] Complexes with one disubstituted cyclophane ligand.
[e] Complexes with one monosubstituted cyclophane ligand.
[f] Not determined due to strong overlap of peaks.

in Table 3, together with the peak potential separation ΔE_p for the two peaks of the couple. All potential values are referred to the ferrocene/ferricinium standard redox couple [40] in the respective solvent. Hence, values from experiments in different solvents are comparable. In the present case, these $\bar{E}$ cannot simply be interpreted as formal potentials for the overall two-electron process, since E_p^{red} and E_p^{ox} possibly belong to different electron transfer steps. Moreover, the distortions due to adsorption hamper the comparability of the $\bar{E}$. However, the values still indicate the relative ease of the redox reactions of the respective complexes.

Earlier work had identified both electronic (electron density of aromatic deck attached to Ru^{2+}) and structural (flexibility of ligand and ease to attain a boat shaped geometry in η^4-ligation) influences on the redox potential of Ru complexes with arene ligands [13,28,29]. These conclusions were based on complexes with HMB, benzene, and various cyclophanes as ligands. With the complexes investigated in the present report, compounds with electron-withdrawing substituents in the cyclophane moiety are available for the first time, and can be compared to ethenyl- and unsubstituted complexes.

Some general observations derived from the $\bar{E}$ for the Ru complex reduction processes are discussed in the following.

The HMB complexes are reduced at more negative potentials than the corresponding [2$_2$](1,4)cyclophane compounds [see, $\bar{E}$(**6**) vs. $\bar{E}$(**7**), $\bar{E}$(*anti*-**10a**) vs. $\bar{E}$(*anti*-**12a**), $\bar{E}$(*anti*-**10b**) *vs.* $\bar{E}$(*anti*-**12b**), and $\bar{E}$(**11b**) vs. $\bar{E}$(**13b**)]. This is in accordance with the behavior of **2** and **3** already documented [24,29]. The difference between the redox potential for **2** and **3** was attributed to the increased flexibility of the Ru cyclophane ligand as compared to HMB.

Moreover, the *syn*- and the di-substituted complexes are more easily reduced than the standard compounds **2** and **3** without substituents in the cyclophane ligands, and the ethenyl substituted complexes **6**, **7**, and **4**, respectively. However, the anti-complexes surprisingly exhibit $\bar{E}$ values more negative than the unsubstituted parent compounds. *anti*-**10b** forms the only exception with an $\bar{E}$ slightly positive of $\bar{E}$(**2**). The disubstituted complexes are reduced more easily than the *syn*-monosubstituted compounds. These facts speak against electronic effects as sole explanation of $\bar{E}$ shifts in these cases. Although the electron-withdrawing power is certainly attenuated for a substituent in the *anti*-deck, we would still expect a decrease of electron density at the Ru^{2+} central atom, and, consequently, less negative $\bar{E}$ than for the unsubstituted compound.

Structural effects, on the other hand, may be present due to the substituents in the aromatic decks. For example, the methacrylic substituents should favor the tendency of the attached aromatic deck to attain an out-of-plane distorted conformation. Indeed, there is a small but significant increase in the out-of-plane angle in the cyclophane adjacent to the substituent (see, X-ray results for the ligands, above). Preformation of such a conformation in the complexing deck (*syn*) supports the reduction, which must result in a η^4-ligated cyclophane.

In contrast, an out-of-plane distortion at the *anti*-deck may render the complexing arene ring less flexible, and, consequently, reduction becomes more difficult. In the di-substituted complexes the *syn*-deck is already in a favorable conformation and the electronic effects of the two substituents seem to control $\bar{E}$.

Finally, we observe that the ester complexes are more easily reduced than their acid counterparts (cf. **11a/11b,** *anti*-**10a/10b,** *syn*-**and** *anti*-**12a/12b**). In the framework of structural effects discussed, the smaller COOH groups as compared to $CO(OC_2H_5)$ exert less drastic effects.

The values of ΔE_p at $v = 0.1$ V s^{-1} range from 33 to 127 mV. For **3** Boekelheide et al. [24] had reported $\Delta E_p = 134$ mV. Due to the overlap of the peaks from two closely spaced one-electron redox processes, the larger ΔE_p values can not be taken as indication of slow electron transfers, since the maxima of the reductive and the oxidative currents correspond to peaks from two different redox events. For a one-electron system, a minimum of $\Delta E_p = 58$ mV is expected under diffusion control [41]. The lower values of ΔE_p found here, thus indicate the presence of a two-electron system with a difference of formal potentials below $\Delta E^0 = 30$ mV, and possibly, potential inversion [42].

2.9. Oxidation

Oxidation of Ru arene complexes had first been observed for the ethenyl substituted compounds **4**, **6**, and **7**, close to the anodic limit in a CH_2Cl_2 electrolyte [31]. Similarly, complexes **10**–**13** are oxidized at relatively high potentials, above $\approx +1.2$ V in DCB. No true peaks develop in the cyclic voltammograms (see Fig. 5 for the example of **10b**), but the current increases significantly above its background value. On repeated cycling the changes in appearance of the current/potential curves is striking.

The potential was first scanned into a negative direction from the rest potential of the electrolyte (no current; $E \approx -0.25$ V). In the first cycle, the redox reactions assigned to the reduction of Ru^{2+} (Eq. (1)) is observed. Upon scanning E to positive values, a broad wave is found at $E > 1$ V. During a second scan to -1.4 V, the original reduction signal is already severely distorted at both GC and Pt. At Pt additional broad peaks appear at $E = 0$ to -0.8 V. The broad oxidation

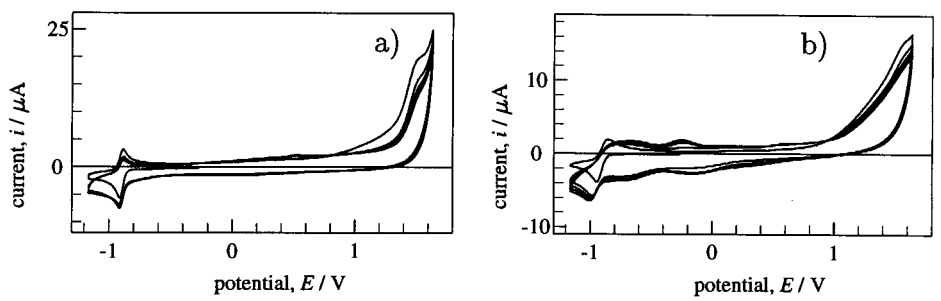

Fig. 5. Multi-cycle voltammograms of *anti*-**10b** (conditions as in Figure 4) including oxidation of the starting compound; (a) GC; (b) Pt as electrode material.

wave of the starting compound decreases during a multi-cycle experiment. The new waves, however, increase from cycle to cycle. These signals are not of the typical shape found for freely diffusing species, but rather resemble those of adsorbed or surface confined species. Moreover, the large width at half height indicates repulsive interactions between these species.

We thus assume that upon anodic oxidation the methacrylate ester and methacrylic acid substituted Ru arene complexes form a redox-active film on the electrode surface, and thus modify the electrode, in particular in the case of Pt as the electrode material. Further experiments to elucidate the nature and characteristics of these films are currently under way in our laboratory.

3. Conclusions

Methacrylate ester and methacrylic acid substituted $[2_2]$(1,4)cyclophanes react with Ru^{2+} acetone solvates under mild reaction conditions (no CF_3COOH) to form ruthenium arene sandwich type complexes. The compounds synthesized in this work present the first examples of $[2_2]$(1,4)cyclophanes with such polar, electron-withdrawing substituents and their organometallic complexes. The NMR spectroscopic and reductive electrochemical behavior can be understood on the basis of that observed for more simple cyclophanes and Ru arene complexes, but with additional steric and electronic effects. Finally, electrochemical oxidation leads to modification of the electrode surface with electroactive films.

4. Experimental

4.1. General

Elemental analyses were performed with a Carlo Erba (Modell 1106) instrument. Mass spectra were obtained with a Finnigan MAT TSQ 70 quadrupol-instrument (ion source temperature 200°C , electron energy 70 eV) for EI and a Finnigan MAT 771A for FD (ion source temperature 30°C). FAB spectra were obtained with the latter instrument (NBA Matrix, ion source temperature 50°C). The standards for the calibration of the high resolution mass spectra were $P[(C_6H_6)_3]_2Au$, or, for the higher molecular mass compounds, suitably chosen complexes from our series.

NMR spectra were measured on a Bruker AMX400 (400 MHz) spectrometer with standard techniques and programs. C,H correlations were performed using the phase sensitive TPPI sequence preceded by an inverse BIRD pulse to suppress signals from protons bound to ^{12}C.

NMR spectra of the ligands were recorded in $CDCl_3$, except those of **8a** (this compound was investigated in both $CDCl_3$ and d_6-DMSO), and **9a** (soluble only in d_5-pyridine and, to a limited extent, in d_6-DMSO). The NMR spectra of the complexes were recorded in CD_3NO_2, in d_6-DMSO, or in d_6-acetone. All shift values are given versus TMS.

Melting points were determined in capillary tubes.IR specta were recorded on a Jasco FTIR-430 spectrometer in KBr.

4.2. Crystallography

Intensities were collected with ω-scan on an ENRAF Nonius CAD4 diffractometer using $Cu-K_\alpha$ radiation ($\lambda = 1.54184$ Å) at 233 K. All calculations were performed using the SHELX93 package. The structures were solved by direct methods. All non-hydrogen atoms were refined anisotropic. The hydrogen atoms have been determined in the difference Fourier map and were refined isotropic. The refinement of the coordinates and the anisotropic thermal parameters of the non-hydrogen atoms was carried out by the full matrix least squares method against F^2. The final R indices and other parameters are given in Table 1.

4.3. Syntheses

4.3.1. Syntheses of ligands

4.3.1.1. General. 1,2,4,5-Hexatetraene [43] and propynal [44] were prepared according to literature procedures. Their reaction to 4,12-di-formyl-$[2_2]$(1,4)cyclophane (**16**) and conversion of this dialdehyde to **17** was described by Hopf and coworkers [34,45].

*4.3.1.2. E-4-(2′-ethoxycarbonyl-2′-methyl)ethenyl-$[2_2]$-(1,4)cyclophane (**8b**).* A total of 1 g (44 mmol) of sodium metal was disolved under an argon atmosphere in 10 ml of absolute ethanol. 1.9 g (7.5 mmol; 1.73 ml) of 96% triethyl-2-phosphonopropionate (Lancaster, Mühlheim, Germany) were added and the mixture was stirred for 15 min. A suspension of 118 mg (0.5 mmol) of 4-formyl-$[2_2]$(1,4)cyclophane in 20 ml of absolute ethanol was added over a period of 30 min. and the mixture was stirred at room temperature (r.t.) for 17 h until the thin layer chromatogram (silica; ethyl acetate–petroleum ether (30/50) = 1:2) showed only the product spot. A yellow precipitate formed after addition of water (150 ml) and was extracted three times with 50 ml of dichloromethane. The combined dichloromethane fractions were washed with water and dried with magnesium sulfate overnight. The drying agent was filtered off and the solution was concentrated to a volume of 20 ml. The product was purified with column chromatography over silica (ethyl acetate–petroleum ether (30/

50) = 1:2) to give 132 mg (83 %) of **8b** (colorless crystals; m.p. 110°C).

Anal. Calc. for $C_{22}H_{24}O_2$ C, 82.46; H, 7.55. Found C, 82.45; H, 7.49%. IR: 1710 (s, C=O, val.), 1640 (m, C=C, val.), 1260/1240 (s, C–O, val.). MS (EI): 320 [M^+, 40%], 215 (100%), 142 (85%), 104 (75%).

^{1}H-NMR ($CDCl_3$): $\delta = 7.66$ ppm (s, vinyl, 1H), 6.32–6.62 (arom., 7H), 4.29 (q, CH_3CH_2, 2H), 2.77–3.36(m, ethano, 8H), 1.86 (d, CH_3, 3H), 1.37 (t, CH_3CH_2, 3H). ^{13}C-NMR ($CDCl_3$): $\delta = 168.75$ ppm (s, COOEt), 139.42 (s, vinyl), 128.33–139.58 (arom.), 60.80 (s, CH_3CH_2), 33.86–35.14 (s, ethano), 14.44 (s, CH_3), 14.04 (s, CH_3CH_2).

*4.3.1.3. E-4-(2′-carboxy-2′-methyl)ethenyl-[2$_2$](1,4)cyclophane (**8a**).* A total of 400 mg (1.25 mmol) of 4-(2-ethoxycarbonyl-2′-methyl)ethenyl-[2$_2$](1,4)cyclophane (**8b**) was suspended in 25 ml of ethanol. After adding a solution of 600 mg (11 mmol) KOH in 20 ml of ethanol the mixture was boiled under reflux for 3 h. The formation of the acid was controlled by thin layer chromatography (silica; 98:2 dichloromethane–ethyl acetate). The product mixture was added to 30 ml of water. In order to precipitate the acid, 1 ml of concentrated hydrochloric acid was added dropwise to the solution. Instantly the product precipitated as colorless solid which was extraced three times with 50 ml of dichloromethane. The collected dichloromethane solutions were dried with anhydrous magnesium sulfate. The drying agent was filtered off and the solvent was evaporated. Vapor diffusion with acetone and petroleum ether (30/50) yielded 305 mg (84 %) of **8a** (colorless crystals ; m.p. 211°C).

Anal. Calc. for $C_{20}H_{20}O_2$ C, 82.16; H, 6.89. Found C, 82.18; H, 6.97%. IR: 3000 (m, COO-H, val), 1680 (s, C=O, val), 1620 (m, C=C, val). MS (EI): 292 [M^+, 20%], 187 (40%), 147 [$M^+ - CO_2$, 70%], 104, (100%) ^{1}H-NMR ($CDCl_3$): $\delta = 12.48$ ppm (d_6-DMSO, s, COOH, 1H), 7.82 (s, vinyl, 1H), 6.38–6.62 (arom., 7H), 2.81–3.41 (m, ethano, 8H), 1.91 (d, CH_3, 3H). ^{13}C-NMR ($CDCl_3$): $\delta = 174.03$ ppm (s, COOH), 140.74 (s, vinyl), 127.03–139.62 (arom.), 33.71–35.28 (s, ethano), 13.59 (s, CH_3).

*4.3.1.4. 4,12-Di-[E-(2′-(ethoxycarbonyl)-2′-methyl-ethenyl]-[2$_2$](1,4)cyclophane (**9b**).* Under an argon atmosphere sodium metal (0.5 g, 22 mmol) was dissolved in 10 ml of absolute ethanol. After addition of 722 mg (3 mmol; 0.66 ml) of 96% triethyl-2-phosphono propionate (Lancaster, Mühlheim, Germany) the mixture was stirred for 15 min. A suspension of 200 mg (0.76 mmol) of 4,12-di-formyl-[2$_2$](1,4)cyclophane in 20 ml of absolute ethanol was added over a period of 30 min and the mixture was stirred at r.t. for 24 h until thin layer chromatography (silica; 30:50 ethyl acetate–petroleum ether (30/50) = 1:2) showed only the product spot. After addition of water (200 ml) the product was extracted three times with 60 ml of dichloromethane. The combined dichloromethane fractions were washed with water and dried over night with magnesium sulfate. The drying agent was filtered off and the solution was concentrated to a volume of 20 ml. The latter was passed through a silica column (ethyl acetate–petroleum ether (30/50) = 1:2). The resulting solution was evaporated to give 250 mg (76%) of **9b** (colorless crystals; m.p. 137°C).

Anal. Calc. for $C_{28}H_{32}O_4$ C, 77.75, H, 7.45; Found: C, 77.54; H, 7.36%. IR: 1700 (s, C=O, val), 1640 (m, C=C, val), 1270/1230 (s, C–O, val). MS (EI): 432 [M^+, 15%], 215 (75%), 143 (100%), 104 (10%). ^{1}H-NMR ($CDCl_3$): $\delta = 7.68$ ppm (s, vinyl, 2H), 6.37–6.61 (arom., 6H), 4.31 (q, CH_3CH_2, 4H), 2.86–3.28(m, ethano, 8H), 1.86 (d, CH_3, 6H), 1.38 (t, CH_3CH_2, 6H). ^{13}C-NMR ($CDCl_3$): $\delta = 168.60$ ppm (s, COOEt), 138.23 (s, vinyl), 128.53–139.20 (arom.), 60.74 (s, CH_3CH_2), 33.16–34.10 (s, ethano), 14.31 (s, CH_3), 13.93 (s, CH_3 CH_2).

*4.3.1.5. 4,12-Di-[E-(2′-carboxy)-2′-methyl-ethenyl]-[2$_2$](1,4)cyclophane (**9a**).* A total of 95 mg (0.22 mmol) of 4,12-bis-[(2′-ethoxycarbonyl-2′-methyl)-ethenyl]-[2$_2$](1,4)cyclophane (**9b**) was suspended in 10 ml of ethanol. After adding a solution of NaOH (340 mg, 8.5 mmol) in 15 ml of ethanol the mixture was boiled under reflux for 2 h. The formation of the product was controlled by thin layer chromatography (silica; 98:2 dichloromethane–ethyl acetate). After boiling, 30 ml of water were added to the mixture. In order to precipitate the acid, 1 ml of concentrated hydrochloric acid was added dropwise to the solution. The resulting solid was filtered off, washed with 2 ml of ether, dried, and redissolved in a solution of 100 mg NaOH in 10 ml of water. Precipitation with 1 ml of concentrated hydrochloric acid, washing with 2 ml of ether and finally drying under vacuum gave a yield of 64 mg (77%) of **9a** (colorless solid; m.p. > 350°C under decomposition).

Further purification was achieved by the vapor diffusion technique with pyridine and ethylacetate.

Anal. Calc. for $C_{24}H_{24}O_2$ C, 76.57; H, 6.43. Found: C, 75.01; H, 5.49%. IR: 2939 (m, COO–H, val.), 1689 (s, C=O, val.), 1635 (m, C=C, val.). MS (FD): 376 [M^+, 100%]. ^{1}H-NMR (d_5-pyridine): $\delta = 12.52$ ppm (d_6-DMSO, s, COOH, 2H), 8.22 (s, vinyl, 2H), 6.49–6.77 (arom., 6H), 2.78–3.39 (m, ethano, 8H), 2.14 (d, CH_3, 6H). ^{13}C-NMR (d_5-pyridine): $\delta = 169.55$ ppm (s, COOH), 136.79 (s, vinyl), 128.69–138.29 (arom.), 32.03–34.24 (s, ethano), 13.13 (s, CH_3).

4.3.2. Syntheses of complexes

4.3.2.1. General. Bis(HMB)dichlorobis(μ-chloro)-diruthenium(II) [39,46] or di-μ-chloro-bis[(η^6-[2$_2$](1,4)cyclophane)-chlororuthenium(II)] [24] and silver tetrafluoro-

borate were stirred in 2.5 or 3 ml acetone for 30 or 60 min, respectively. The precipitated silver chloride was removed by filtration and washed two times with acetone. After concentration of the combined filtrates to a volume of 2 ml, the solid substituted cyclophane ligand was added. The mixture was boiled under reflux. Upon cooling to room temperature, a yellow precipitate formed in most cases, which was collected by filtration and washed with 20 ml of ether. In the cases of **11b** and **13b,** the product was precipitated from the solution by addition of diethylether (150 ml).

The ruthenium complexes were purified by vapor diffusion crystallization with the solvents indicated below. The raw product was dissolved in 2 ml of a suitable solvent, e.g. acetone. Insoluble material was removed by filtration. A flask with the filtrate was placed in a tank with ether. After several days at −20°C, yellow crystals formed at the glass walls and were separated from additional dark and amorphous material. If needed, this procedure was repeated several times. Regioisomers could not always be separated completely by this procedure, the isomer ratio, however, varied from recrystallisation to recrystallisation. Isomeric ratios given in the following are for the products of the first crystallization. The ratios were determined from ^{1}H-NMR spectra, comparing the integrated signals of the HMB ligand (HMB complexes) or the vinyl protons ([2$_2$](1,4)cyclophane complexes). As observed before in similar cases, [31] the ruthenium complexes melt under decomposition with a melting behavior which is not useful for characterization. Satisfactory elemental analyses of the complexes could not be obtained, possibly due to the presence of Ru and F in the samples.

[**11**–**16**-η^6-*E*-4-(2′-ethoxycarbonyl-2′-methyl)-ethenyl-[2$_2$](1,4)cyclophane] - (η^6 - hexamethylbenzene) - ruthenium(II)bis(tetrafluoroborate) *anti*-**10b** and [**3**–**8**-η^6-*E*-4-(2′-ethoxycarbonyl-2′-methyl)-ethenyl-[2$_2$](1,4)cyclophane](η^6 - hexamethylbenzene)–ruthenium(II)bis(tetrafluoroborate) *syn*-**10b** were prepared from 25 mg (0.038 mmol) of bis(HMB)dichlorobis(μ-chloro)-diruthenium(II), 30 mg (0.15 mmol) of silver tetrafluoroborate and 24 mg (0.075 mmol) of **8b**. The reaction time under reflux was 5 h. Yield: 38 mg (67%; from ether and acetone) of a 4.5:1 mixture of *anti*-**10b** to *syn*-**10b**. 15 mg of the pure *anti* isomer were isolated after diffusion of ether into a dichloromethane solution of this mixture.

MS (high resolution) *m*/*e* Calc. for $C_{34}H_{42}O_2BF_4Ru$, 671.22575. Found 671.22761. IR: 1699 (s, C=O, val.), 1629 (m, C=C, val.), 1263/1223 (s, C–O, val.). *anti*-**10b**: ^{1}H-NMR (CD_3NO_2): $\delta = 7.47$ ppm (s, vinyl, 1H), 6.27–7.05 (m, arom., 7H), 4.25 (q, CH_3CH_2, 2H), 3.21–3.66 (m, ethano, 8H), 2.53 (s, HMB, 18H), 1.81 (d, CH_3, 3H), 1.31 (t, CH_3CH_2, 3H). ^{13}C-NMR (CD_3NO_2): $\delta = 171.02$ ppm (COOH), 137.78 (vinyl), 90.97–138.74 (arom.), 64.35 (CH_2), 33.09–36.12 (ethano), 19.53 (HMB), 16.25 (CH_3), 16.16 (CH_3CH_2). *syn*-**10b**: ^{1}H-NMR (CD_3NO_2): $\delta = 7.34$ ppm (s, vinyl, 1H), 6.52–6.79 (m, arom., 7H), 4.37 (q, CH_3CH_2, 2H), 2.46 (s, HMB, 18H), 1.37 (t, CH_3CH_2, 3H).

[**11**–**16**-η^6-*E*-4-(2′-carboxy-2′-methyl)-ethenyl-[2$_2$]-(1,4)cyclophane] [η^6-hexamethylbenzene)–ruthenium-(II)bis(tetrafluoroborate) *anti*-**10a** was prepared from 26 mg (0.038 mmol) of bis(HMB)dichlorobis(μ-chloro)–diruthenium(II), 30 mg (0.15 mmol) of silver tetrafluoroborate and 24 mg (0.08 mmol) of **8a**. The reaction time under reflux was 5 h. Yield: 24 mg (41%; from ether and acetone) of *anti*-**10a**.

MS (high resolution) *m*/*e* Calc. for $C_{32}H_{38}O_2BF_4Ru$ 643.19444. Found: 643.19344. IR: 3068 (m, COO–H, val.), 1706 (s, C=O, val.), 1625 (w, C=C, val.). ^{1}H-NMR (CD_3NO_2): $\delta = 12.78$ ppm (d_6-DMSO, s, COOH, 1H), 7.61 (s, vinyl, 1H), 5.86–6.98 (m, arom., 7H), 3.0–3.21 (ethano, 8H), 2.32 (s, HMB, 18H), 1.83 (s, CH_3, 3H). ^{13}C-NMR (CD_3NO_2): $\delta = 168.88$ ppm (COOH), 134.96 (vinyl), 88.25 −135.31 (arom.), 29.53–32.84 (ethano), 16.88 (HMB), 14.01 (CH_3).

[**11**–**16**-η^6-4,12-Di[*E*-(2′-ethoxycarbonyl-2′-methyl)-ethenyl]-[2$_2$](1,4)cyclophane][η^6-HMB]-ruthenium(II)-bis(tetrafluoroborate) (**11b**) was prepared from 50 mg (0.075 mmol) of bis(HMB)dichlorobis(μ-chloro)-diruthenium(II), 59 mg (0.3 mmol) of silver tetrafluoroborate and 65 mg (0.15 mmol) of **9b**. The reaction time under reflux was 6 h. Yield: 57 mg (82%; from ether and acetone) of **11b**. MS (high resolution) *m*/*e* Calc. for $C_{40}H_{50}O_4BF_4Ru$ 783.28022; Found 783.2923; the deviation between the experimental and the expected values is larger here than in the other cases due to matrix effects.

IR: 1706 (s, C=O, val.), 1632 (w, C=C, val.), 1261 (s, C–O, val.). ^{1}H-NMR (CD_3NO_2): $\delta = 7.72$ ppm (s, *anti*-vinyl, 1H), 7.01 (s, *syn*-vinyl, 1H), 5.97–7.08 (arom., 6H), 4.39 (q, *syn*-CH_3CH_2, 2H), 4.36 (q, *anti*-CH_3CH_2, 2H), 3.17–3.35 (m, ethano, 8H), 2.39 (s, HMB, 18H), 2.51 (d, *syn*-CH_3, 3H), 1.87 (d, *anti*-CH_3, 3H), 1.39 (t, *syn*-CH_3CH_2, 3H), 1.34 (t, *anti*-CH_3CH_2, 3H).

^{13}C-NMR (CD_3NO_2): $\delta = 169.48$ ppm (*anti*-COOEt), 167.87 (*syn*-COOEt), 136.42 (*anti*-vinyl), 126.54 (*syn*-vinyl), 88.0–136.49 (arom.), 63.04 (*syn*, and *anti*-CH_2), 31.48–34.06 (s, ethano), 17.75 (HMB), 15.75 (*syn*-CH_3), 14.73 (*anti*-CH_3), 14.60 (*syn*-CH_3CH_2), 14.52 (*anti*-CH_3CH_2).

[**11**–**16**-η^6-4,12-Di[*E*-(2′-carboxy-2′-methyl)-ethenyl]-[2$_2$](1,4)cyclophane] [η^6-HMB]–ruthenium(II)bis(tetrafluoroborate) (**11a**) was prepared from 50 mg (0.093 mmol) of bis(HMB)dichlorobis(μ-chloro)-diruthenium(II), 72 mg (0.37 mmol) of silver tetrafluoroborate and 70 mg (0.19 mmol) of **9a**. The reaction time under reflux was 6 days. Yield: 50 mg (32%; from ether and dichloromethane) of **11a**.

MS (high resolution) *m/e* Calc. for $C_{36}H_{42}O_4Ru$ 639.20483. Found: 639.21148. IR: 2960 (s, COOH, val.), 1700 (s, C=O, val.), 1635 (w, C=C, val.). ^{1}H-NMR (d_6-DMSO): $\delta = 12.87$ (s, broad, COOH, 2H), 7.96 ppm (s, *anti*-vinyl, 1H), 7.11 (s, *syn*-vinyl, 1H), 6.39–7.19 (arom., 6H), 3.16–3.56 (m, ethano, 8H), 2.73 (s, HMB, 18H), 2.60 (d, *syn*-CH_3, 3H), 1.96 (d, *anti*-CH_3, 3H). ^{13}C-NMR (CD_3NO_2): $\delta = 167.92$ ppm (COOH), 134.33 (*anti*-vinyl), 125.14 (*syn*-vinyl), 91.12–140.96 (arom.), 29.34–36.15 (ethano), 17.56 (HMB), 15.11 (*syn*-CH_3), 13.99 (*anti*-CH_3).

[η^6-[2$_2$](1,4)cyclophane][**11**–**16**-η^6-*E*-4-(2′-ethoxycarbonyl-2′-methyl)-ethenyl-[2$_2$](1,4)cyclophane]-ruthenium(II)bis(tetrafluoroborate) *anti*-**12b** and [η^6-[2$_2$]-(1,4)cyclophane] [**3**–**8**-η^6-*E*-4-(2′-ethoxycarbonyl-2′-methyl)-ethenyl-[2$_2$](1,4) cyclophane]–ruthenium(II) bis (tetrafluoroborate) *syn*-**12b** were prepared from 71 mg (0.093 mmol) of di-μ-chloro-bis-[(η^6-[2$_2$](1,4)cyclophane)–chlororuthenium(II), 73 mg (0.37 mmol) of silver tetrafluoroborate and 60 mg (0.19 mmol) of **8b**. The reaction time under reflux was 7 h. Yield: 86 mg (58 %; twice from ether and dichloromethane) of a 7:1 mixture of *anti*-**12b**:*syn*-**12b**.

MS (high resolution) *m/e* Calc. for $C_{38}H_{40}O_2BF_4Ru$ 717.21009. Found: 717.20777. IR: 1730 (s, C=O, val.), 1630 (m, C=C, val.), 1262 (s, C–O, val.). ^{1}H-NMR (CD_3NO_2): $\delta = 7.56$ ppm (s, vinyl, 1H), 5.82–7.0 (m, arom., 15H), 4.28 (q, CH_3 CH_2, 2), 2.97–3.55 (m, ethano, 8H), 1.81 (d, CH_3, 3H), 1.30 (t, *anti*-CH_3CH_2, 3H), 1.08 (t, *syn*-CH_3CH_2). ^{13}C-NMR (CD_3NO_2): $\delta =$ 170.97 ppm (COOH), 137.05 (vinyl), 86.67–146.97 (arom.), 62.82 (CH_2), 32.4–35.13 (ethano), 14.71 (CH_3), 14.62(CH_3CH_2).

[η^6-[2^2](1,4) cyclophane][**11**–**16**-η^6-*E*-4-(2′-carboxy-2′-methyl)-ethenyl]-[2$_2$](1,4) cyclophane)–ruthenium(II)-bis(tetrafluoroborate) *anti*-**12a** and [η^6-[2$_2$](1,4)cyclophane][**3**–**8**-η^6-*E*-4-(2′-carboxy-2′-methyl)-ethenyl[2$_2$]-(1,4)cyclophane] – ruthenium(II)bis(tetrafluoroborate)-*syn*-**12a** were prepared from 71 mg (0.093 mmol) of di-μ-chloro-bis-[(η^6-[2$_2$](1,4)cyclophane)chlororuthenium-(II)], 73 mg (0.37 mmol) of silver tetrafluoroborate and 55 mg (0.19 mmol) of **8a**. The reaction time under reflux was 24 h. Yield: 28 mg (19%; from ether and acetone) of a 2.2:1 mixture of *anti*-**12a**:*syn*-**12a.**

MS (high resolution) *m/e* Calc. for $C_{36}H_{36}O_2BF_4Ru$ 689.1879. Found 689.18774. IR: 3050 (s, COO–H, val.), 1690 (s, C=O, val.), 1586 (w, C=C, val.).

^{1}H-NMR (CD_3NO_2): $\delta = 12.64$ ppm (d_6-DMSO, s, COOH, 1H), 7.61 (s, vinyl, 1H), 5.88–7.0 (m, arom., 15H), 2.86–3.4 (m, ethano, 8H), 2.06 (d, *anti*-CH_3, 3H), 1.82 (d, *syn*-CH_3). ^{13}C-NMR (CD_3NO_2): $\delta =$ 170.73 ppm (COOH), 135.41 (vinyl), 85.60–135.1 6(arom.), 33.69–35.5 (ethano), 14.26 (s, CH_3).

(η^6-[2$_2$](1,4)cyclophane)(**11**–**16**-η^6-4,12-bis[*E*-(2′ethoxycarbonyl-2′-methyl)-ethenyl]-[2$_2$](1,4)cyclophane)–ruthenium(II)bis(tetrafluoroborate) **13b** was prepared from 70 mg (0.093 mmol) of di-μ-chloro-bis-[(η^6-[2$_2$](1,4)cyclophane)chlororuthenium(II), 73 mg (0.37 mmol) of silver tetrafluoroborate and 83 mg (0.19 mmol) of **9b**. The reaction time under reflux was 6 h. Yield: 89 mg (51%; from ether and dichloromethane) of **13b**.

MS (high resolution) *m/e* Calc. for $C_{44}H_{48}O_4BF_4Ru$ Calc. 829.26256. Found: 829.25552. IR: 1706 (s, C=O, val.), 1634 (w, C=C, val.), 1261 (s, C–O, val.).

^{1}H-NMR (CD_3NO_2): $\delta = 7.64$ ppm (s, *anti*-vinyl, 1H), 7.03 (s, *syn*-vinyl, 1H), 5.87–6.99 (m, arom., 14H), 4.25 (m, CH_2, 4H), 2.96–3.31 (m, ethano, 8H), 2.29 (d, *syn*-CH_3, 3H), 1.82 (d, *anti*-CH_3, 3H), 1.34 (t, *syn*-CH_3CH_2, 3H), 1.31 (t, *anti*-CH_3CH_2, 3H).

^{13}C-NMR (CD_3NO_2): $\delta = 169.36$ ppm (*anti*-COOEt), 167.83 (*syn*-COOEt), 136.22 (*anti*-vinyl), 128.19 (*syn*-vinyl), 87.06–136.39 (arom.), 62.13–62.79 (*syn*- and *anti*-CH_2), 32.24–35.14 (ethano), 15.97 (CH_3, two strongly overlapping peaks for *syn* and *anti*), 14.72 (*syn*-CH_3CH_2), 14.57 (*anti*-CH_3CH_2).

4.4. Electrochemical experiments

4.4.1. Solvents and supporting electrolyte

Activation of Al_2O_3 for solvent drying: Al_2O_3 was activated by heating neutral Al_2O_3 (Macherey & Nagel, Düren, Germany) at 400°C and 2×10^{-4} mbar for 2 h. The activated drying agent was stored under an argon atmosphere.

Purification of 1,2-dichloro benzene (DCB)*:* 1 l of 1,2-dichlorobenzene (Merck–Schuchardt, Hohenbrunn, Germany) was stirred two times with 50 ml of sulfuric acid (98%) for 24 h, washed three times with 100 ml of water and dried over anhydrous $CaCl_2$. After filtration the solvent was purified by distillation (b.p. 81–82°C/40 mbar) over CaH_2. To remove traces of water, the 1,2-dichlorobenzene was stored over activated Al_2O_3.

Purification of acetonitrile: Acetonitrile (Merck–Schuchardt, Hohenbrunn, Germany) was predried over $CaCl_2$ for at least a week. The solvent was then distilled over P_2O_5, CaH_2 and again P_2O_5 under Ar. Finally, the solvent was passed through a column with activated Al_2O_3.

Purification of dimethylsulfoxide [47]: 250 ml of DMSO (Merck–Schuchardt, Hohenbrunn, Germany) were stirred with 20 g of NaOH at 90°C for 1 h, followed by distillation (b.p. 52–54°C/0.6 mbar). 5 g of CaH_2 were added and the solvent was again distilled.

Purification of propylene carbonate (PC) was performed as described earlier [31]. Tetra-*n*-butylammonium hexafluorophosphate, NBu_4PF_6, was prepared from NBu_4Br and NH_4PF_6 (Fluka) in analogy to the procedure given [48]. The supporting electrolyte was used in a concentration of 0.1 M, except for the experiments in DCB. In the latter case, 0.06 M solutions of the supporting electrolyte were used due to solubility

reasons. The electrolyte was degassed by three freeze–pump–thaw cycles before transferring it into the electrochemical cell under argon.

4.4.2. Equipment

All electrochemical experiments were performed with a Bioanalytical Systems (BAS, West Lafayette, IN, USA) 100 B/W electrochemical workstation controlled by a standard 80486 processor based personal computer (control program version 2.0). For electroanalytical experiments a BAS Pt or glassy carbon (GC) electrode tip was used as the working electrode [electroactive areas: 0.070 ± 0.004 mm^2 (GC electrode; from experiments in CH_3CN and CH_2Cl_2; standard deviation between the experiments in the two solvents); 0.062 ± 0.001 mm^2 (Pt electrode; from experiment in CH_3CN; standard deviation given is for various scan rates)]. The electroactive areas of the disks were determined from cyclic voltammograms of ferrocene under the assumption of a diffusion coefficient $D(\mathrm{fc},CH_2Cl_2) = 2.32 \times 10^{-5}$ cm^2 s^{-1} [49] or $D(\mathrm{fc},CH_3CN) = 2.4 \times 10^{-5}$ cm^2 s^{-1} [11]. The counter electrode was a Pt wire (diameter: 1 mm).

In all experiments, the reference electrode was a Ag/Ag^+ [0.01 M $AgClO_4$/0.1 M NBu_4PF_6 in CH_3CN] electrode, connected to the cell via a Haber–Luggin double reference construction [50]. Ferrocene was used as an external standard [40]. Its potential was determined by separate cyclic voltammetric experiments in the respective solvent. All potentials reported in this paper are rescaled to $E^0(\mathrm{fc/fc^+}) = +0.266$ V (vs. the Ag/Ag^+ reference for 1,2-dichlorobenzene), $+0.086$ V (acetonitrile), or $+0.036$ V (DMSO) and thus given versus the $\mathrm{fc/fc^+}$ redox potential.

For cyclic voltammetry a gas-tight full-glass three-electrode cell as described before [48] was used. The cell was purged with argon before being filled with the electrolyte. Background curves were recorded before adding the substrate to the electrolyte. The background currents were later subtracted from the experimental data measured in the presence of substrate. No iR compensation was performed.

5. Supplementary material

Crystallographic data (excluding structure factors) for the structures reported in this paper have been deposited with the Cambridge Crystallographic Data Centre as supplementary publications no. CCDC-134190 (**9b**) and CCDC-134191 (**8a**). Copies of the data can be obtained free of charge on application to CCDC, 12 Union Road, Cambridge CB2 1EZ, UK (fax: +44-1223/336-033; e-mail: deposit@ccdc.cam.ac.uk).

Acknowledgements

The authors thank the Deutsche Forschungsgemeinschaft, Bonn-Bad Godesberg, Germany (Heisenberg fellowship for BS; SPP 'Elektrochemische Grundlagen der Nanotechnologie'; Graduiertenkolleg 'Chemie in Interphasen') and the Fonds der Chemischen Industrie, Frankfurt/Main, Germany, for financial support. We are indepted to Degussa AG, Frankfurt/Main, for gifts of ruthenium trichloride and Pt wire, to V. Boekelheide, Eugene/OR, USA, for a gift of [2$_2$](1,4)cyclophane, and H. Hopf, Braunschweig, Germany, for providing us with details of the synthetic procedure leading to compounds **15** and **18**, as well as samples of **16** and **17**. B. Krauß is acknowledged for determining the mid-point potentials of **2** and **3** during work on his diploma thesis. We thank M.E. Maier, Tübingen, for the use of his FT-IR spectrometer.

References

[1] B. Speiser, S. Dümmling, in: J. Russow, G. Sandstede and R. Staab (Eds.), Elektrochemische Reaktionstechnik und Synthese — Von den Grundlagen bis zur industriellen Anwendung, 1999, pp. 33–39.
[2] G. Wilkinson, J. Am. Chem. Soc. 74 (1952) 6146.
[3] P.G. Gassman, C.H. Winter, J. Am. Chem. Soc. 110 (1988) 6130.
[4] I. Chávez, A. Cisternas, M. Otero, E. Román, U. Müller, Z. Naturforsch. Teil B 45 (1990) 658.
[5] I. Chávez, M. Otero, E. Román, U. Müller, J. Organomet. Chem. 427 (1992) 369.
[6] E. Lindner, I. Krebs, R. Fawzi, M. Steimann, B. Speiser, Organometallics 18 (1999) 480.
[7] M.A. Bennett, T.W. Matheson, J. Organomet. Chem. 175 (1979) 87.
[8] M.A. Bennett, T.-N. Huang, T.W. Matheson, A.K. Smith, Inorg. Synth. 21 (1982) 74.
[9] J.A. Page, G. Wilkinson, J. Am. Chem. Soc. 74 (1952) 6149.
[10] M.G. Hill, W.M. Lamanna, K.R. Mann, Inorg. Chem. 30 (1991) 4687.
[11] T. Kuwana, D.E. Bublitz, G. Hoh, J. Am. Chem. Soc. 82 (1960) 5811.
[12] E.O. Fischer, C. Elschenbroich, Chem. Ber. 103 (1970) 162.
[13] R.G. Finke, R.H. Voegeli, E.D. Laganis, V. Boekelheide, Organometallics 2 (1983) 347.
[14] D.T. Pierce, W.E. Geiger, J. Am. Chem. Soc. 111 (1989) 7636.
[15] D.T. Pierce, W.E. Geiger, J. Am. Chem. Soc. 114 (1992) 6063.
[16] G. Huttner, S. Lange, Acta Crystallogr. Sect. B 28 (1972) 2049.
[17] S. Suravajjala, J.R. Polam, L.C. Porter, J. Organomet. Chem. 461 (1993) 201.
[18] S. Suravajjala, J.R. Polam, L.C. Porter, Organometallics 13 (1994) 37.
[19] K.-D. Plitzko, V. Boekelheide, Angew. Chem. 99 (1987) 715; Angew. Chem. Int. Ed. Engl. 26 (1987) 700.
[20] K.-D. Plitzko, G. Wehrle, B. Gollas, B. Rapko, J. Dannheim, V. Boekelheide, J. Am. Chem. Soc. 112 (1990) 6556.
[21] V. Boekelheide, Pure Appl. Chem. 58 (1986) 1.
[22] E.D. Laganis, R.G. Finke, V. Boekelheide, Tetrahedron Lett. 21 (1980) 4405.
[23] W.D. Rohrbach, V.B. Boekelheide, J. Org. Chem. 48 (1983) 3673.

[24] R.T. Swann, A.W. Hanson, V. Boekelheide, J. Am. Chem. Soc. 108 (1986) 3324.
[25] V. Boekelheide, Top. Curr. Chem. 113 (1983) 87.
[26] E. Heilbronner, Z.Z. Yang, Top. Curr. Chem. 115 (1983) 1.
[27] F. Gerson, Top. Curr. Chem. 115 (1983) 57.
[28] T. Satou, K. Takehara, M. Hirakida, Y. Sakamoto, H. Takemura, H. Miura, M. Tomonou, T. Shinmyozu, J. Organomet. Chem. 577 (1999) 58.
[29] E.D. Laganis, R.H. Voegeli, R.T. Swann, R.G. Finke, H. Hopf, V. Boekelheide, Organometallics 1 (1982) 1415.
[30] K.-D. Plitzko, B. Rapko, B. Gollas, G. Wehrle, T. Weakley, D.T. Pierce, W.E. Geiger Jr., R.C. Haddon, V. Boekelheide, J. Am. Chem. Soc. 112 (1990) 6545.
[31] B. Gollas, B. Speiser, J. Sieglen, J. Strähle, Organometallics 15 (1996) 260.
[32] S. Dümmling, B. Gollas, B. Speiser, manuscript in preparation.
[33] B. Gollas, I. Hesse, R. Lotz, H. Pasch, B. Speiser, I. Zagos, Liebigs Ann./Recueil (1997) 2255.
[34] E. Herrmann, Synthese und Polymerisation von Vinylderivaten des [2.2]Paracyclophans, PhD thesis, Technische Hochschule Braunschweig, 1990.
[35] G. Gallagher Jr., R.L. Webb, Synthesis (1974) 122.
[36] E. Pretsch, T. Clerc, J. Seibl, W. Simon, Tabellen zur Strukturaufklärung organischer Verbindungen mit spektroskopischen Methoden, third ed., Springer, Berlin, 1986.
[37] B. Gollas, B. Speiser, J. Sieglen, J. Strähle, C. Maichle-Mössmer, Z. Krist. 212 (1997) 271.
[38] T. Sato and K. Torizuka, J. Chem. Soc. Perkin II (1978) 1199.
[39] S.L. Grundy, P.M. Maitlis, J. Chem. Soc. Chem. Commun. (1982) 379.
[40] G. Gritzner, J. Kůta, Pure Appl. Chem. 56 (1984) 461.
[41] R.S. Nicholson, I. Shain, Anal. Chem. 36 (1964) 706.
[42] D.H. Evans, K. Hu, J. Chem. Soc. Faraday Trans. 92 (1996) 3983.
[43] H. Hopf, I. Böhm, J. Kleinschroth, Org. Synth. Coll. VII (1990) 485.
[44] J.C. Sauer, Org. Synth. Coll. IV (1963) 813.
[45] H. Hopf, personal communication.
[46] M.A. Bennett, T.W Matheson, G.B. Robertson, A.K. Smith, P.A. Tucker, Inorg. Chem. 19 (1980) 1014.
[47] J.F. Coetzee (Ed.), Recommended Methods for Purification of Solvents and Tests for Impurities, Pergamon, Oxford, 1982.
[48] S. Dümmling, E. Eichhorn, S. Schneider, B. Speiser, M. Würde, Curr. Sep. 15 (1996) 53.
[49] J.B. Cooper, A.M. Bond, J. Electroanal. Chem. 315 (1991) 143.
[50] B. Gollas, B. Krauß, B. Speiser, H. Stahl, Curr. Sep. 13 (1994) 42.